ANALYSIS OF NATURAL CIRCULATION TESTS IN THE EXPERIMENTAL FAST REACTOR JOYO

Nabeshima K, Doda N, and Ohshima H
Fast Reactor Computational Engineering Department
Japan Atomic Energy Agency (JAEA)
4002 Narita-cho, O-arai-machi, Higashi-ibaraki-gun, Ibaraki, 311-1393, JAPAN
nabeshima.kunihiko@jaea.go.jp; doda.norihiro@jaea.go.jp; ohshima.hiroyuki@jaea.go.jp

Mori T and Ohira H
Monju Project Management and Engineering Center
Japan Atomic Energy Agency (JAEA)
1 Shiraki, Tsuruga-shi, Fukui 919-1279, JAPAN
mori.takero@jaea.go.jp; ohira.hiroaki@jaea.go.jp

Iwasaki T
NESI Inc.
4002 Narita-cho, O-arai-machi, Higashi-ibaraki-gun, Ibaraki, 311-1313, JAPAN
iwasaki.takashi57@jaea.go.jp

ABSTRACT

Natural circulation is one of the most important mechanisms to remove decay heat in the sodium cooled fast reactors from the viewpoint of passive safety. The fast reactors can be designed to enable core cooling with natural circulation induced by the temperature difference of the coolant without any forced convection by the circulation pumps. On the other hand, it is difficult to evaluate plant dynamics accurately under low flow natural circulation condition. In JAEA, plant dynamics simulation code Super-COPD has been developed to analyze DBEs/BDBEs of sodium cooled fast reactors. In this study, Super-COPD has been validated through the application to the analysis of natural circulation tests in the experimental fast reactor JOYO with Mark-II irradiation core.
Almost all plant components in JOYO including four air-coolers were modeled in Super COPD so as to focus on the simulation accuracy of natural circulation behavior in the reactor core, the primary and secondary system. Furthermore, the full scale modeling of fuel subassembly was also adopted in this analysis. The natural circulation test after reactor scram from 100MW full power at JOYO was selegted and simulated by Super-COPD. The computational results were compared with the measured temperature and flow fields. The transient behaviors predicted by Super-COPD showed good agreement with the experimental data.

KEYWORDS
fast reactor, JOYO, plant dynamics analysis, natural circulation, decay heat removal

1. INTRODUCTION

One of the advantages of sodium-cooled fast reactors is high capability of natural circulation decay heat removal due to the large difference between core outlet and inlet temperatures. Decay Heat Removal

System (DHRS) utilizing natural circulation is highly reliable because it does not depend on active components such as pump, blower, and electric power supply. Therefore, it's free from the need for high-capacity power load or quick activation of emergency power supplies even in the case of the loss of all AC power such as the accident at TEPCO's Fukushima Daiich nuclear power station.

Several kinds of transient tests were conducted in the Japanese experimental fast reactor JOYO to demonstrate the capability of decay heat removal by natural circulation. Here, we focus on 100MW transient test which was performed in 1986 under Mark-II irradiation core conditions [1]. The test was initiated by tripping primary and secondary sodium pumps manually, and then the reactor was shut down simultaneously. The plant-wide dynamic codes SSC-L [2] and MIMIR-N2 [3] were already applied to the analysis of this natural circulation transient test at JOYO. Theses codes could predict the thermal hydraulic behaviors using appropriate boundary conditions, although all of the plant components in JOYO were not modeled. For example, it was impossible for SSC-L to simulate the two different loops at the same time. MIMIR-N2 could model only one air cooler for each loop. In this study, we carried out numerical simulation of the test using a plant dynamics analysis code Super-COPD [4],[5] to confirm its applicability to the natural circulation phenomena. Here, almost all components in JOYO including each fuel subassembly in the core and four air-coolers were modeled in Super-COPD.

The schematic representation of JOYO plant is shown in Fig. 1. JOYO is a two-loop system: Loop-A and Loop-B are shown on the left- and the right−hand side in Fig. 1, respectively. The primary side of JOYO consists of the reactor core, shell side of intermediate heat exchangers (IHXs), primary coolant pumps, check valves and heat transfer piping systems. The secondary side consists of heat transfer tubes of IHXs, dump heat exchangers (DHXs), secondary coolant pumps and piping systems. Two DHXs (Air-Coolers) are installed in each secondary loop as the heat sink. The thermal power generated in the reactor core is finally transferred to the air in decay heat removal operation as well as the normal full power operation.

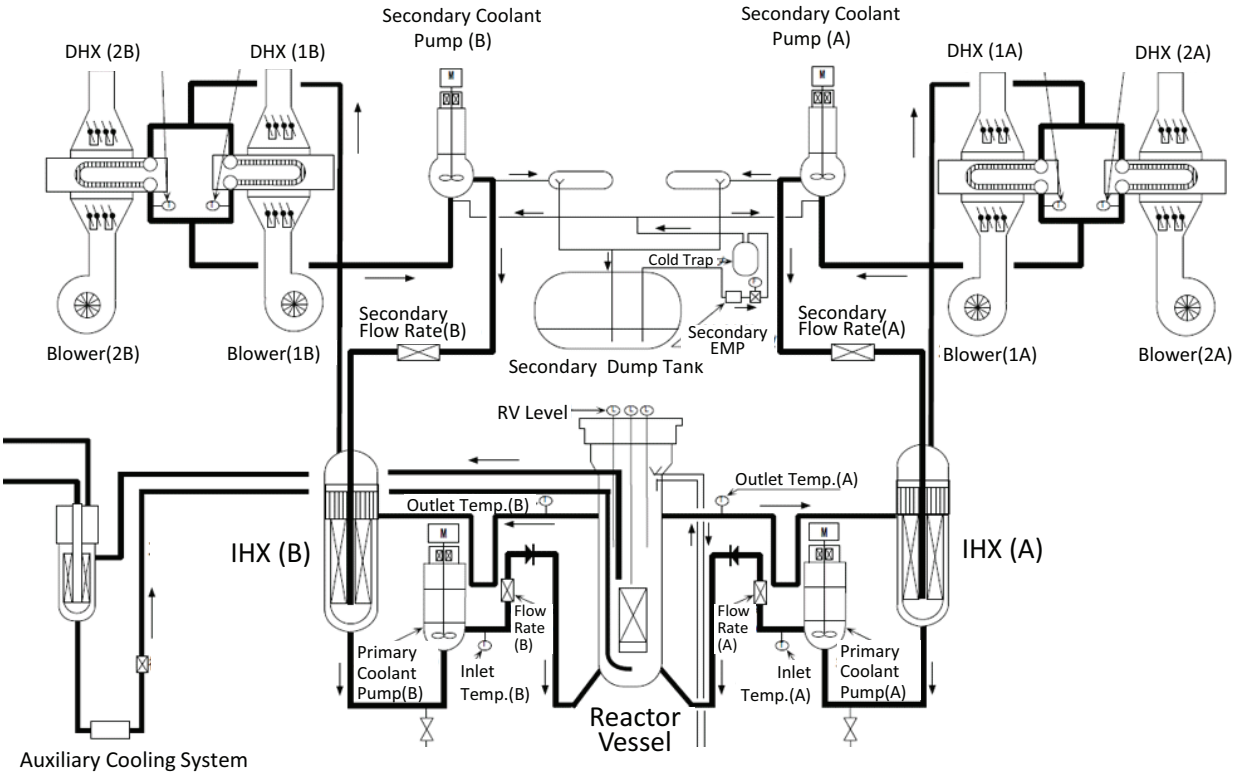

Figure 1. Schematic representation of JOYO.

The main thermal hydraulic characteristics of JOYO with Mark-II irradiation core is shown in Table I. The rated thermal power is 100MW. Although there is no difference between the two primary loops, hot-leg and cold-leg temperatures of the secondary loop are slightly different between Loop-A and Loop-B. It's because the design specifications of Loop-A's IHX are not exactly the same as those of Loop-B's IHX. For example, the number and the diameter of heat transfer tubes and bypass flow rate in the IHX are different. Therefore, the hot-leg and cold-leg temperatures in Loop-A are higher than those in Loop-B during the normal operation. The temperature difference between the hot-leg and cold-leg in Loop-A is 4.4 ^{o}C higher than that in Loop-B. On the other hand, the coolant mass flow rate in Loop-A is 28 ton/h less than that in Loop B. In Super-SOPD code, the influence of the asymmetry of two IHXs can be easily modeled as two different modules.

At the beginning of the transient test, the primary coolant pumps, the secondary coolant pumps and the overflow electric magnetic pump (EMP) were manually stopped simultaneously just after scram. On the other hand, the model of the auxiliary cooling system was not considered in the analysis because the auxiliary coolant pump was already stopped before the test. The transients of flow rates and coolant temperatures in primary and secondary loops were measured and recorded for 10,000 sec. The numerical simulation results by Super-COPD are compared with these measured data.

Table I. Main characteristics of JOYO

Plant Parameter		unit
Thermal Power	100	MW
Number of Loops	2	
Primary Coolant Flow Rate	1,085	ton/h/loop
Primary Hot-Leg Temperature	497.3	^{o}C
Primary Cold-Leg Temperature	368.4	^{o}C
Secondary Loop (Loop-A)		
Coolant Flow Rate	1,098	t/h
Hot-Leg Temperature	457.6	^{o}C
Cold-Leg Temperature	332.1	^{o}C
Temperature Difference	125.5	^{o}C
Secondary Loop (Loop-B)		
Coolant Flow Rate	1,126	t/h
Hot-Leg Temperature	470.8	^{o}C
Cold-Leg Temperature	349.7	^{o}C
Temperature Difference	121.1	^{o}C
Air-Cooler Mass Flow	1,080	t/h
Air-Cooler Inlet Temperature	20	^{o}C

2. MODEL DESCRIPTION OF THE PLANT DYNAMICS CODE, SUPER-COPD

2.1. Reactor Core of JOYO with Mark-II

The reactor core of JOYO consists of 313 fuel subassemblies (S/A) including 65 fuel assemblies in zero to fifth layer, 46 inner reflectors, 189 outer reflectors, 6 control rods and other components. Four kinds of fuel subassemblies including control rods are modeled in Super-COPD. Figure 2 shows the fuel subassembly configuration of JOYO with Mark-II irradiation core. The zero layer of fuel assembly means it's at the center of the reactor core in the figure. A special fuel assembly was installed in the third layer, and an instrumented test assembly (INTA) was installed in the fifth layer. Most important physical

phenomena in the reactor core during the natural circulation behavior are; flow redistribution, radial heat transfer among the fuel subassemblies and decay heat of the fuel assemblies. However, the previous analyses with representative channel model in the core couldn't simulate those phenomena precisely [2], [3]. Therefore, the full scale modeling of all the 313 fuel subassemblies is implemented by Super-COPD in this analysis. The heat transfer in the radial direction between fuel subassemblies could be modeled by considering thermal resistance of wrapper tube and sodium among fuel subassemblies in Super-COPD.

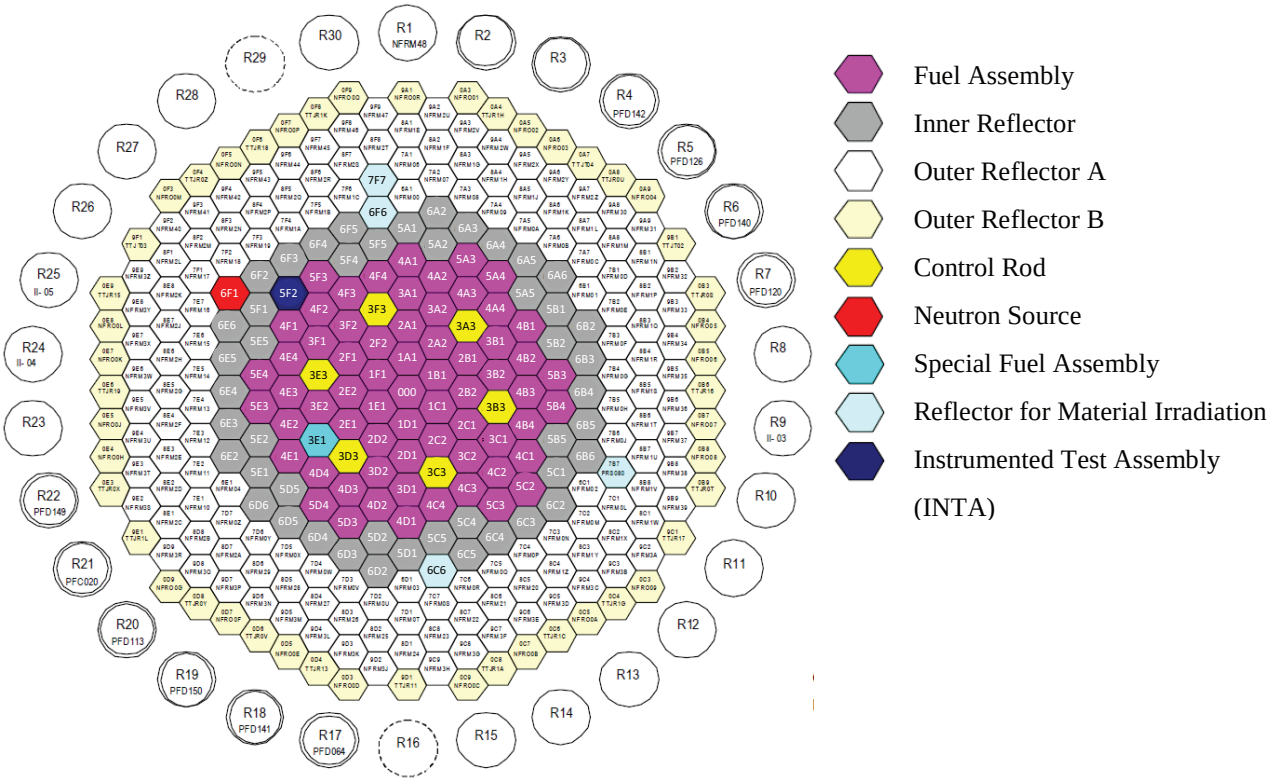

Figure 2. Fuel S/A configuration of JOYO reactor core.

Figure 3 indicates the thermal hydraulic model of reactor core in Super-COPD. The modules in Super-COPD are shown in the square shape. Here, MN and LN in the squares mean mixing tee module and sodium pipe line module, respectively. The circle and rectangle indicate the temperature boundary and the flow rate boundary, respectively. The fuel subassemblies are connected to high pressure plenum through mixing tee. On the other hand, the inner and outer reflectors, control rods and other subassemblies are connected to low pressure plenum through mixing tee. All of fuel subassemblies are connected to the upper-plenum through mixing tee. The model of upper plenum consists of a module although the volume is large. The thermal hydraulic calculation of whole core is performed using the pressure of upper plenum and that of the high pressure plenum inlet in order to evaluate the flow rate and temperature of each fuel subassembly. There is bypass flow between the outside of outer reflectors and reactor vessel wall.

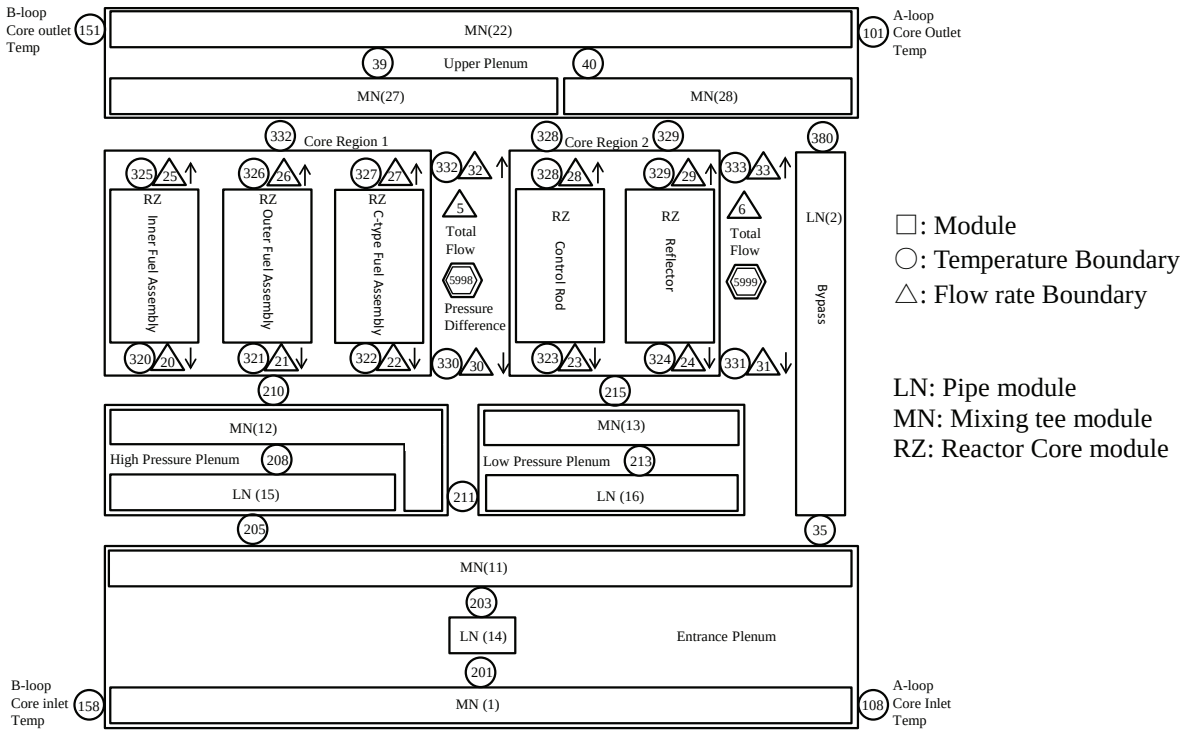

Figure 3. Reactor core thermal hydraulic model.

2.2. Thermal Calculation Model of Primary and Secondary Coolant Loops

Figure 4 shows thermal calculation model of primary and secondary coolant loops, and air coolers in Loop-A. Primary and secondary coolant loops consist of Loop-A and Loop-B. Furthermore, all of four air coolers are modeled in this analysis. The auxiliary cooling system model is not considered.

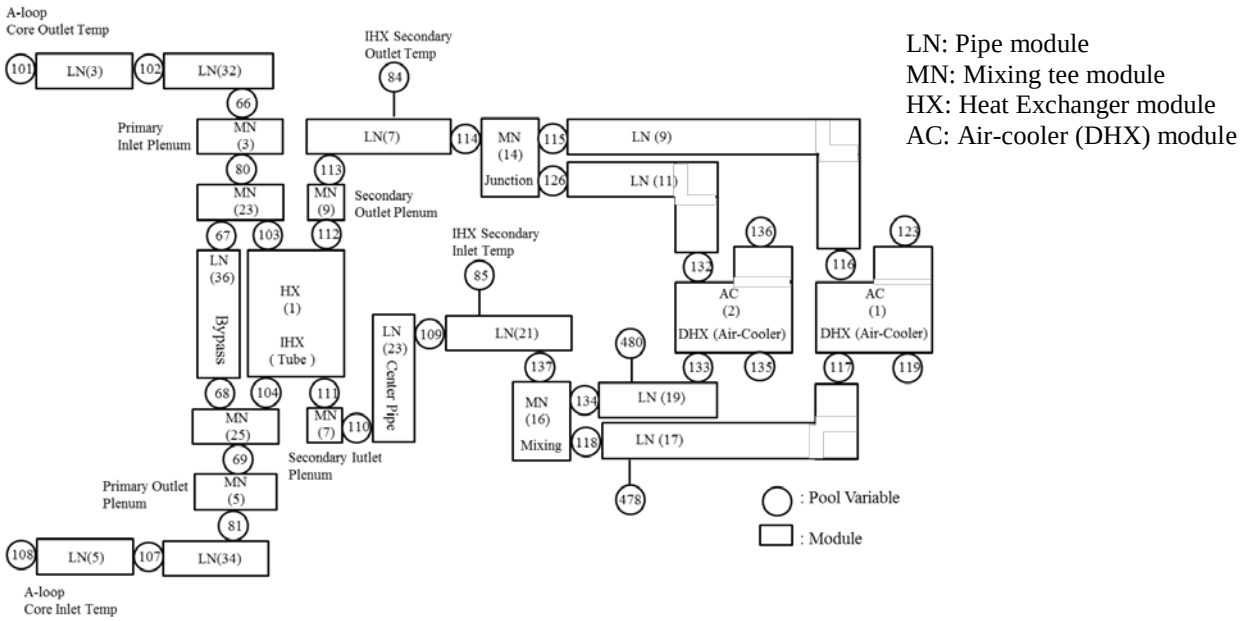

Figure 4. Thermal calculation model of primary and secondary loop (Loop-A).

A model, one heat transfer tube representing the heat transfer part of the IHX and the air cooler, is utilized to determine the axial temperature distribution of the heat transfer tube by solving the one-dimensional axial energy conservation law. Here, the IHX plenum is a complete mixing model. Piping section uses a multi-order lag model that takes into account the heat transfer of the structural material. In this analysis, the heat transfer correlation equation by Subbotin is used for high flow rate, whereas the heat transfer coefficient for the low flow rate is evaluated by the experimental IHX equation using 50MW SG facility [6].

In the flow calculation model of the primary and the secondary cooling systems, the law of conservation of mass and momentum are simultaneously solved by one-dimensional flow network model that takes into account the pressure loss characteristics of the equipment and piping, valve characteristic, circulation pump characteristic and natural circulation force to calculate the flow rate, liquid level and pressure of the coolant. In the flow calculation model at the air side of air cooler, the air flow rate is calculated by solving pressure drop characteristics of the vane damper and in/outlet duct, and momentum conservation law in consideration of the main blower characteristics and natural circulation force. The boundary condition of the analysis is the air side inlet temperature at the air coolers.

3. CALCULATION RESULTS

3.1. Temperature Transient of Reactor Core

The coolant temperature distribution in the core before the scram is shown in the diagram at the left end of Figure 5. The temperature difference between the zero layer and the second layer fuel assemblies is more than 30 ^{o}C during 100MW stable state operation because of the forced convection caused by the circulation pumps. The coolant temperature in fuel subassemblies decreased after the scram, then it increased again by decay heat of fuel. Here, it is clear that the maximum temperature difference among fuel subassemblies became about 25 ^{o}C at the second peak (around 150 seconds) because of the heat transfer in the radial direction during natural circulation. The temperature in the core was slightly decreased after the second peak.

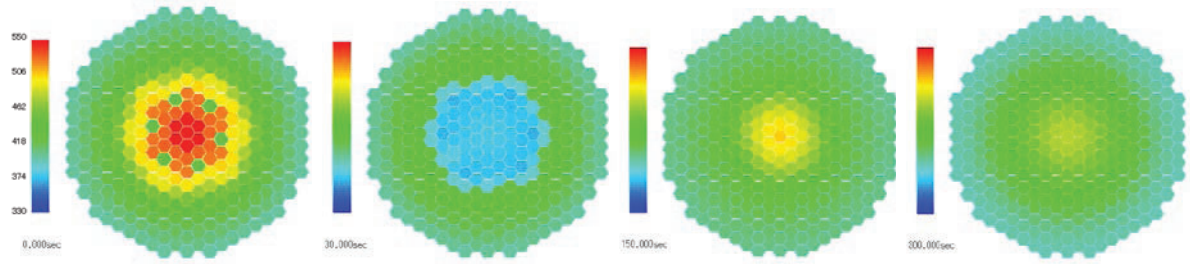

Figure 5. Temperature Distribution of reactor core.

Figure 6 shows the outlet temperature transient of fuel assemblies at zero layer and second layer for 300 second after the scram. The black solid lines indicate the measured values at the experiment. The red line indicates the outlet temperature signal of fuel assembly at zero layer calculated by Super-COPD. The other colored lines indicate the calculated temperature signals of fuel assemblies at second layer. The identifiers in the figure correspond to that of fuel assemblies in Fig. 2. The measured and calculated values of initial temperature are almost same. The measured and calculated values of minimum temperature after the scram are also similar. The calculated second peak temperature is almost same as the measured value around 150 seconds point, although the simulated behavior is 10 second slower than measured one. Those results means the transient behavior of reactor core could be precisely simulated by Super-COPD with full scale modeling of fuel subassemblies.

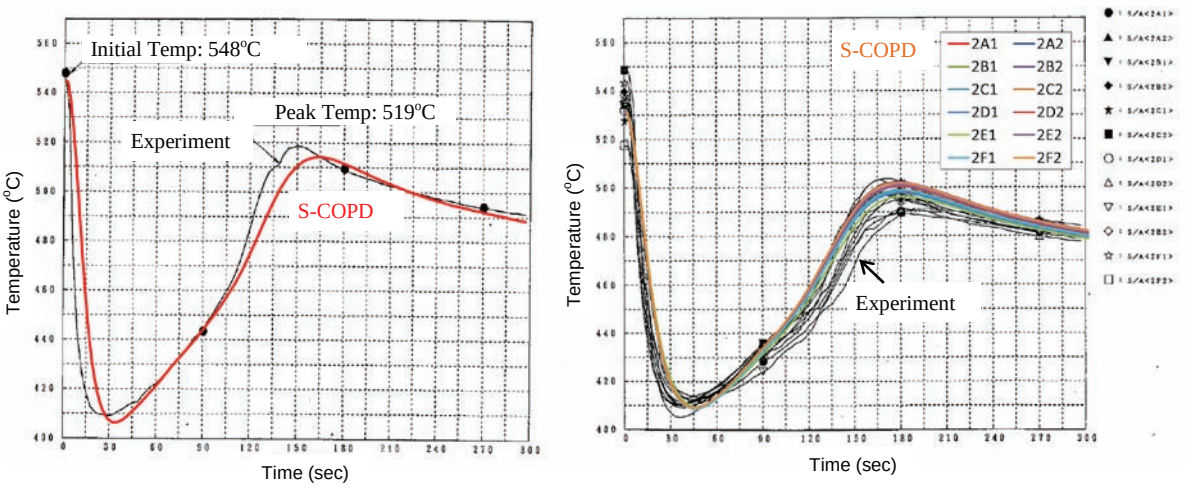

(a) Fuel Assembly at Zero Layer (b) Fuel Assemblies at Second Layer

Figure 6. Outlet temperature transient of fuel assemblies.

3.2. Transient of Primary Loop

Figure 7 shows the measured and calculated temperature signals at reactor core inlet and outlet. The differences between the measured and calculated values at core inlet and outlet are small. Figure 8 shows the measured and calculated flow rate signals at reactor core outlet. The calculated core outlet temperature is slightly lower than measured one because the upper plenum model in Super-COPD is too simple although the volume of the upper plenum of Joyo is large. The decrease of the simulated flow rate after the scram is same as that of experimental value. However, the increase of the simulated flow rate caused by natural circulation is slower than the experimental value, and the behavior is slightly different. It might be due to the difference in the evaluation of heat exchange rate at IHX.

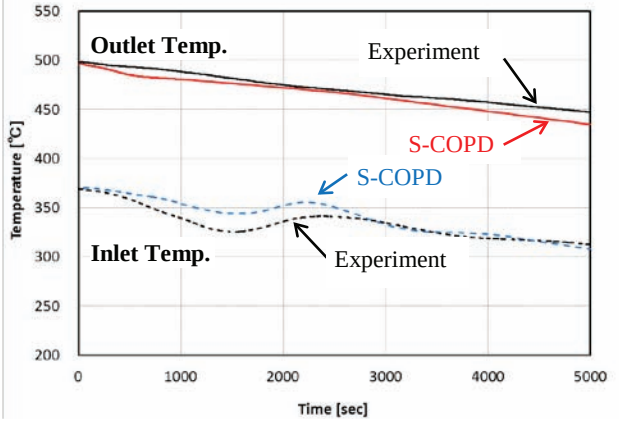

Figure 7. Core inlet and outlet temperature transient.

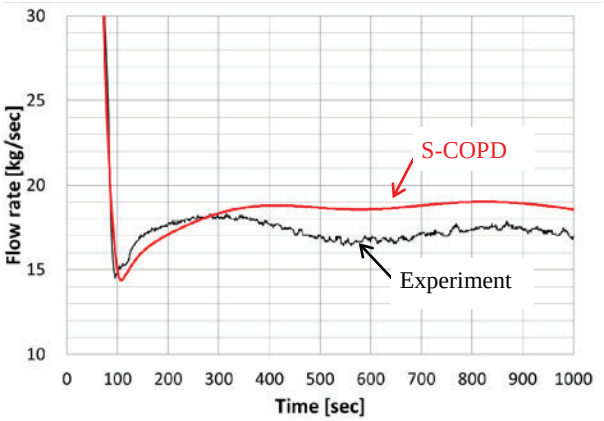

Figure 8. Core outlet flow transient.

3.3. Transient of Secondary Loop

Air flow rate at air side of air cooler was not measured in this experiment. Therefore, the air flow rate is calculated by the rotational speed of blower and the pressure loss. The air side inlet temperature and flow rate at the air coolers are boundary condition of the analysis for normal operation. However, only the air side inlet temperature is boundary condition in this natural circulation test because all blowers are

stopped. Figure 9 shows the inlet and outlet temperature of IHX secondary loop A. The calculated outlet temperature is lower than measured one at the beginning because the calculated pump speed of secondary coolant pump during flow coast down is higher than the actual value. The measured and calculated flow rate signals of secondary loop A are shown in Fig. 10. Both the signals show the same trend. The difference of flow rate after 900 seconds was caused by opening of IHX inlet damper in the reactor coolant temperature control system.

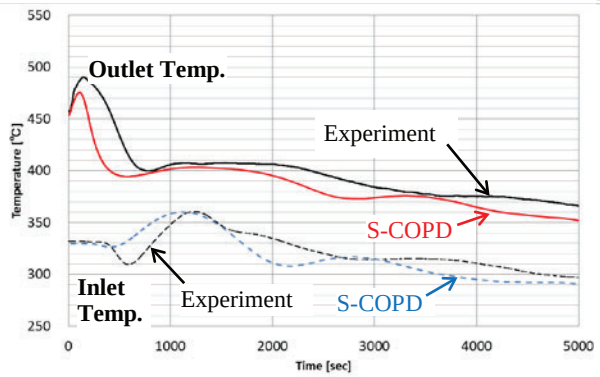

Figure 9. IHX Secondary loop-A temp. transient.

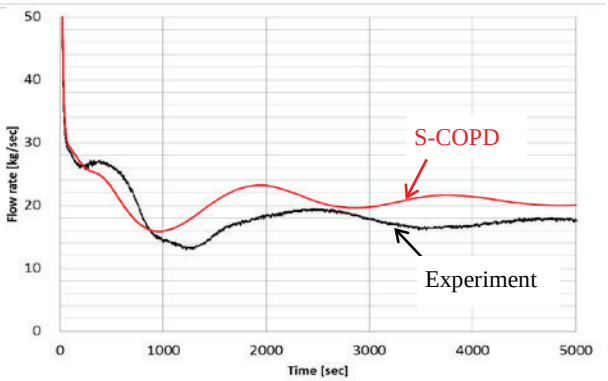

Figure 10. Secondary loop A flow transient.

4. CONCLUSIONS

Fast reactor plant dynamics simulation code Super-COPD has been validated through the application to the analysis of a natural circulation test in the experimental fast reactor JOYO with Mark-II irradiation core. The full scale modeling of all fuel subassemblies were implemented by Super-COPD in this analysis. Furthermore, all of the components in primary and secondary loops including four air coolers were also modeled. 100MW transient data was used as natural circulation test, and the transient behavior of reactor core after the scram could be precisely simulated by Super-COPD. The transient behavior of primary and secondary loops showed almost similar trend. Therefore, it is concluded that the plant dynamics simulation of SFR in the natural circulation transient can be predicted by Super-COPD throughout the whole plant system. Future work for improving accuracy of Super-COPD is to develop more precise upper plenum model and control system of JOYO.

ACKNOWLEDGMENTS

The authors would like to express their sincere gratitude to M. Minami of NESI Inc., for his technical contribution on the modeling and the computational analyses.

REFERENCES

1. T. Aoyama, K. Kinjo, N. Mizoo and F. Asakura, “The Operational Experience of the Experimental Fast Reactor ‘JOYO’”, JAERI-M-92-028, pp. 85-92 (1992).
2. A. Yamaguchi, A. O-iwa and T. Hasegawa, “Plant-wide Thermal Hydraulic Analysis of Natural Circulation Test at JOYO with MK-II Irradiation Core,” *Proceedings of 4th International Topical Meeting on Reactor Thermal-Hydraulics*, Karlsruhe, Germany, October, Vol. 1, pp. 398-405 (1989).
3. M. Sawada, H. Arikawa and N. Mizoo, “Experiment and Analysis on Natural Convection Characteristics in the experimental Fast Reactor JOYO,” *Nucl. Eng. Des.*, **120** (1), pp. 341-347 (1990).

4. F. Yamada, Y. Fukano, H. Nishi and M. Konomura, “Development of Natural Circulation Analytical Model in Super-COPD Code and Evaluation of Core Cooling Capability in MONJU during A Station Blackout,” *Nucl. Tech.*, **188**, pp292-321 (2014).
5. O. Watanabe, K. Oyama, J. Endo, N. Doda, A. Ono, H. Kamide, T. Murakami and Y. Eguchi, “Development of an Evaluation Methodology for the Natural Circulation Decay Heat Removal System in a Sodium Cooled Fast Reactor,” *J. Nucl. Sci. Technol.*, http://dx.doi.org/10.1080/00223131.2014.994049 (2015).
6. H. Mochizuki and M. Takano, “Heat transfer in heat exchangers of sodium cooled fast reactor systems,” *Nucl. Eng. Des.*, **239** (2), pp. 295-307 (2009).